Coupling tumor necrosis factor-related apoptosis-inducing ligand to iron oxide nanoparticles increases its apoptotic activity on HCT116 and HepG2 malignant cells: effect of magnetic core size

Hanene Belkahla, Amranul Haque, Alexander Revzin, Tijani Gharbi, Andrei Alexandru Constantinescu, Olivier Micheau, Miryana Hémadi, Souad Ammar

Journal of Interdisciplinary Nanomedicine

BRITISH SOCIETY FOR NANOMEDICINE

Open Access

Journal of Interdisciplinary Nanomedicine ISSN 2058-3273

ORIGINAL ARTICLE

Coupling tumor necrosis factor-related apoptosis-inducing ligand to iron oxide nanoparticles increases its apoptotic activity on HCT116 and HepG2 malignant cells: effect of magnetic core size

Hanene Belkahla,[1,2,3†] Amranul Haque,[4†,‡,§] Alexander Revzin,[4†,‡,§] Tijani Gharbi,[1†] Andrei Alexandru Constantinescu,[2†] Olivier Micheau,[2*†] Miryana Hémadi[3†] & Souad Ammar[3**†]

[1] *Nanomedicine Lab, Université de Bourgogne Franche-Comté, EA 4662, Besançon, France*

[2] *LNC, Université de Bourgogne Franche-Comté, INSERM UMR-1231, Dijon, France*

[3] *ITODYS, Université Paris Diderot, Sorbonne Paris Cité, CNRS UMR-7086, Paris, France*

[4] *Department of Biomedical Engineering, UC Davis, Davis, California, USA*

Keywords
Cancer nanotherapy, iron oxide nanoparticles, malignant cell death, nanovectors, TRAIL proapoptotic proteins.

Corresponding Authors:
*Olivier Micheau, LNC, Université de Bourgogne Franche-Comté, INSERM UMR-1231, UFR Science de santé, 7 Boulevard Jeanne d'Arc, 21000 Dijon, France.
Fax: +33 -3-80393434; Tel: +33-3-80343468
Email: omicheau@u-bourgogne.fr
**Souad Ammar, ITODYS, Université Paris Diderot, Sorbonne Paris Cité, CNRS UMR-7086, UFR Chimie, 15 rue jean-Antoine de Baïf, 75205 Paris, France.
Fax: +33-1-57277263; Tel: +33-1-57278762
Email: ammarmer@univ-paris-diderot.fr

FUNDING INFORMATION
Agence Nationale de la Recherche (Labex LipSTIC, Labex SEAM, ANR 11 IDEX 05 02, ANR 11 LABX 086, ANR-11-LABX-0021-01); Fondation ARC; Commissariat à l'Investissement d'Avenir

Abstract

Tumor necrosis factor-related apoptosis-inducing ligand (TRAIL) has been considered as a potential anticancer agent owing to its selectivity for malignant cells. However, its clinical use remains limited because of its poor efficacy. Attempts to increase its antitumor activity include, among others, its functionalization by nanoparticles (NPs). In the present study, TRAIL was grafted onto magnetic spinel iron oxide NPs of defined core size, 10 and 100 nm on average, to see whether the size of the resulting nanovectors, NV10 and NV100, respectively, might affect TRAIL efficacy and selectivity. Apoptosis induced by NV10 and NV100 was higher than by TRAIL alone in both HCT116 and HepG2 cells. At equimolar concentrations, neither the nanovectors nor the corresponding NPs displayed cytotoxicity towards normal primary hepatocytes or TRAIL receptor-deficient HCT116 cells. NV100 exhibited superior proapoptotic activity than NV10, as evidenced by methylene blue and annexin V staining. Consistently, both caspase activation and TRAIL death-induced signaling complex formation, as assessed by immunoblot analysis, were found to be increased in cells treated with NV100 as compared with NV10 or TRAIL alone. These results suggest that the size of NPs is important when TRAIL is vectorized for cancer therapy.

Received: 15 September 2018;
Revised: 08 January 2019;
Accepted: 18 January 2019

**Journal of Interdisciplinary Nanomedicine,
2019; 4(1), doi: 10.1002/jin2.55**

†The current address of this author is the same than its affiliation during the paper submission.
‡The actual address of this author is Just Inc., 2000 Folsom St., San Francisco, 94110 California, USA.
§The actual address of this author is Department of Physiology & Biomedical Engineering, Mayo Clinic, Rochester, 55905 Minnesota, USA.

Introduction

There is an enormous potential for applying nanotechnology to drug delivery (Bharti et al., 2015; Douziech-Eyrolles et al., 2007; Kreuter, 2004; Whelan and Mayenne, 2006). The idea is to use a functionalized nanoparticle (NP) vector, which contains the therapeutic agent and is capable of targeting specific diseased cells. This approach is being explored for cancer treatment (Sachdeva, 1998), in order to overcome drug resistance (Baird and Kaye, 2003) and side effects on healthy cells (Alexiou et al., 2005). For this purpose, magnetic drug targeting, where the active agent is attached to a magnetic carrier, is being increasingly investigated. Such a carrier allows concentrating the drug, which can be driven to a defined target site by local application of an external direct current magnetic field. This approach offers also the possibility of monitoring drug delivery by magnetic resonance imaging (MRI) (Jain et al., 2008), improving drug release, or increasing the functionality of the grafted antitumor by magnetic hyperthermia (Bear et al., 2016; Rananeh and Dadras, 2015). Magnetic iron oxide NPs, that is, magnetite and maghemite, have attracted the most interest for these applications. They have the right magnetic properties (Laurent et al., 2011) and exhibit relatively low toxicity (Hanini et al., 2011). Consequently, if they are combined with an antitumoral agent, they may provide significant improvements over conventional treatments.

Tumor necrosis factor-related apoptosis-inducing ligand (TRAIL), also known as Apo2L/TRAIL, has received considerable attention as a potential anticancer agent because of its ability to target malignant cells and to selectively induce their apoptosis (Merino et al., 2007; Walczak et al., 1999). TRAIL is a type II transmembrane protein homologous with other members of the tumor necrosis factor family and consists of 281 amino acids (Walczak et al., 1999; Pitti et al., 1996). Whereas membrane-bound TRAIL induces caspase-8-dependent apoptosis in a wide variety of tumor cell lines (Walczak et al., 1999), soluble TRAIL is unable to do so (Schneider et al., 1998). Increasing TRAIL, or TRAIL-mimetic valence, however, restores its proapoptotic potential (Pavet et al., 2010; Holler et al., 2000; Schneider et al., 1997; Seifert et al., 2014a). This form of apoptosis is the result of unique binding between multimeric TRAIL and its cognate death receptors (DR4 and DR5), which are often over-expressed in tumor cells (Almasan and Ashkenazi, 2003). Despite its therapeutic promise, assessment of TRAIL in the clinic has, so far, been disappointing (Micheau et al., 2013). TRAIL short half-life, rapid renal clearance, poor solubility, and a lack of efficient administration modes have been reported when injected alone (Wang, 2008), prompting its combination with carriers such as latex (Kim et al., 2013), liposomes (Seifert et al., 2014b), gold NPs (Huang and Hsu, 2017), or carbon nanotubes (Zakaria et al., 2015). All these engineered TRAIL-based derivatives display higher apoptosis activity than TRAIL alone in most tumor cell lines. Coupling of TRAIL to iron oxide was found to induce apoptosis of glioma cells and the self-renewal of glioma stem cells in vitro and in vivo (Perlstein et al., 2013). These promising results prompted us to explore their ability to target and destroy other malignant cell lines, typically human colon adenocarcinoma (HCT116) and human hepatoblastoma (HepG2) cells, the latter being more resistant to chemotherapy than the former, as first step towards the generalization of this nanotechnological approach. The present study focalizes first on the nanovector (NV)'s magnetic core size effect, as indeed the magnetic properties of iron oxide NPs rely mainly on their size and crystalline quality. Smaller particles have lower blocking temperatures and saturation magnetization, which makes them less valuable for magnetic hyperthermia. To address this issue, we prepared monodisperse 10-nm single crystal and 100-nm polycrystal maghemite NPs (NP10 and NP100, respectively) by the well-known polyol process (Basti et al., 2010). They were then reacted with (3-aminopropyl) triethoxysilane (APTES) to graft amino groups onto their surface (section). These were then bonded to TRAIL

by covalent peptide bonding with the latter's carboxylic groups, to give hybrids designated as NV10 and NV100, respectively. The proapoptotic effects of these two NVs were compared with that of free TRAIL.

Results

Structural and microstructural tumor necrosis factor-related apoptosis-inducing ligand-functionalized nanoparticles characterization

Routine X-ray diffraction analysis of bare and TRAIL-functionalized NPs was performed to confirm that the magnetic cores were not altered by chemical modification of the surface. Typical iron oxide spinel diffraction patterns were recorded for both NPs and NVs; there was no evidence for any variation in the peak position or relative intensity (not shown). X-ray photoelectron spectroscopy was carried out to confirm the immobilization of TRAIL on the surface of NPs in NVs. Characteristic C1s (285 eV), O1s (530 eV) and Fe2p (712 eV) XPS signatures were observed. They signals exhibit, for each NV sample compared with its NP parent, an increase in the intensity of the former and a decrease in that of the latter (Fig. 1). The Fe2p peak is entirely attributed to the iron oxide core, while the C1s and the O1s peaks are mainly assigned to the organic coating of the NPs, namely, TRAIL for the NVs and the polyol residue for the bare NPs. N1s (400 eV) signal is revealed only in the spectra of NVs. It is mainly originated from amino, ammonium, and amido groups of grafted TRAIL. The high-resolution N1s spectra show that the nitrogen peak intensity is greater in NV100 than in NV10 (Fig. 1). Qualitatively, these results confirm that TRAIL is grafted onto the NP surface and that NV100 concentrates much more TRAIL than NV10.

Conventional analytic protein titration based on the Bradford method (Bradford, 1976), thermogravimetry, and routine magnetometry were used to determine the number of TRAIL proteins grafted per particle (section). First, Bradford analysis gave values of about 10 and 10,546 mol per particle for NV10 and NV100, respectively (Table 1). The weight loss in thermogravimetry (Fig. 2), minus that observed for the parent NP, neglecting the contribution of APTES, is assumed to correspond to the TRAIL content. Using this corrected value for both NV10 and NV100 sample leads to a TRAIL grafting content of about 9 and 8763 mol per particle, respectively.

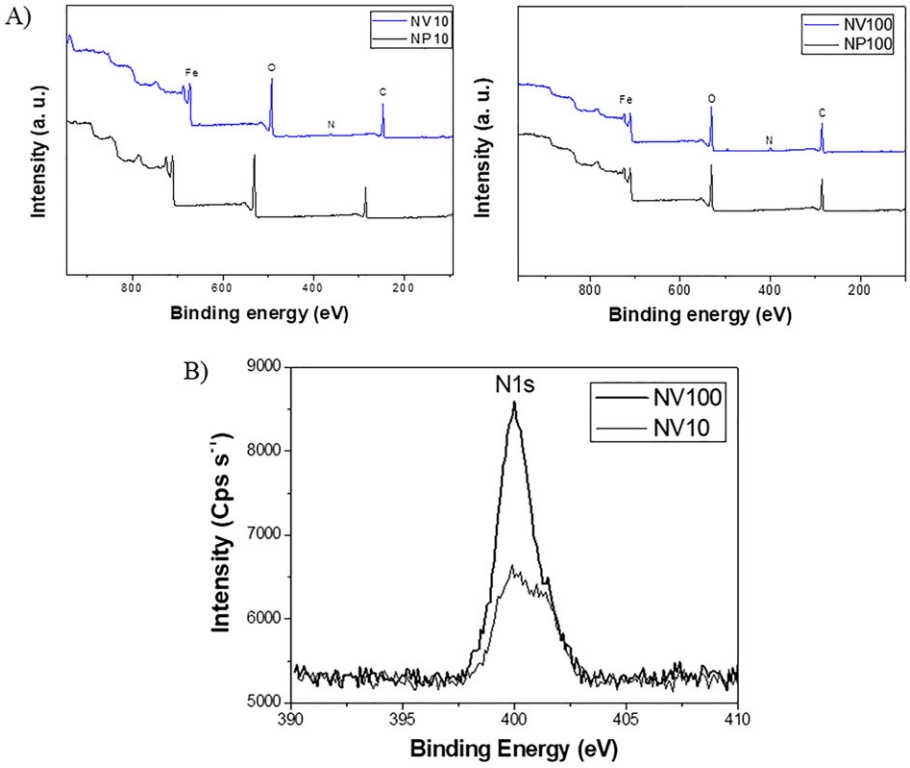

Figure 1. (A) X-ray photoelectron spectroscopy survey spectra of NP10/NV10 and NP100/NV100. (B) The high-resolution of N1s spectra of NV10 and NV100.

Table 1. Quantification of TRAIL grafted on NP10 and NP100 using different techniques: magnetometry analysis, TG analysis, and Bradford assay.

	Magnetometry analysis			TG analysis		Bradford assay
	5K-M_{sat} (emu·g^{-1})	Diamagnetic content (wt.%)	TRAIL content (mol per particle)	Weight loss (wt.%)	TRAIL content (mol per particle)	TRAIL content (mol per particle)
NV10	70.7[†1]	16.2	11	12.0	9	10
NV100	77.6[†2]	8.8	5658	13.8	8762	10,546

TG, thermogravimetry; TRAIL, tumor necrosis factor-related apoptosis-inducing ligand.
[1]To be compared with bare NP10 value 84.3 emu·g^{-1}. [2]To be compared with bare NP100 value 85.1 emu·g^{-1}.

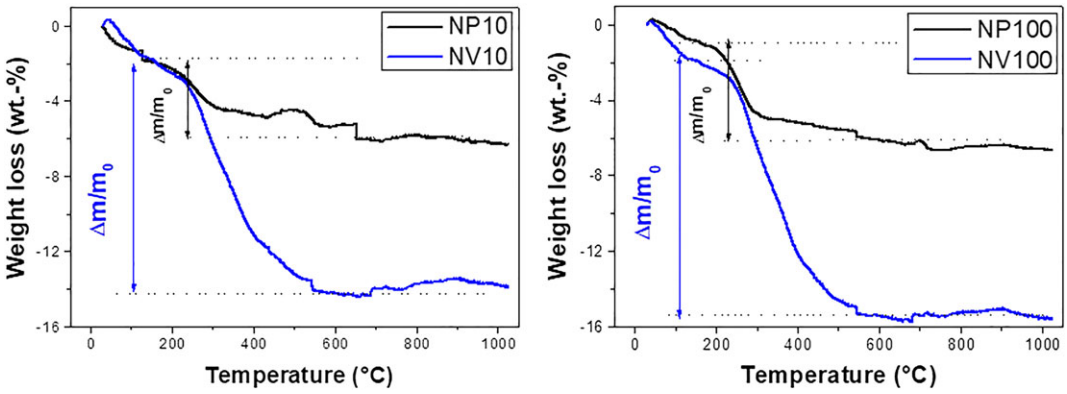

Figure 2. Thermogravimetry analysis of NP10/NV10 and NP100/NV100.

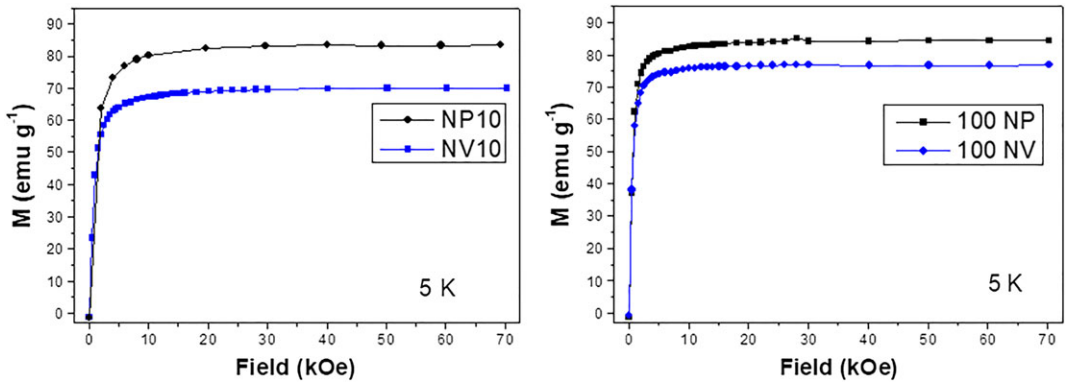

Figure 3. 5K first magnetization curves of NP10/NV10 and NP100/NV100.

Finally, the 5K first magnetization curves of NVs and their parents NPs were plotted (Fig. 3), and the saturation magnetization of each system was determined (per gram of powder). The weight content of TRAIL, *x*, grafted onto NPs was deduced from equation (1), after correction from the diamagnetic APTES contribution (determined by the same method):

$$x.M_{sat}\,(\mathrm{TRAIL}) + (1-x).M_{sat}\,(\mathrm{NPs}) = M_{sat}\,(\mathrm{NVs}), \quad (1)$$

where the saturation magnetizations of free TRAIL (assumed to be zero), bare NPs, and NVs are M_{sat} (TRAIL), M_{sat} (NPs), and M_{sat} (NVs), respectively. The number of TRAIL grafted was found to be about 11 and 5658 mol per particle for NV10 and NV100, respectively, very close to those obtained previously (Table 1).

Therefore, in order to compare the biological properties of all the produced NVs, we performed all the biological assays as a function of TRAIL concentration rather than NV concentration, using the averaged TRAIL content values. In practice, TRAIL, NV, and NP doses were expressed as ligand concentrations in $ng{\cdot}mL^{-1}$. In all the cases, NVs were used at equimolar TRAIL concentrations. In the case of NPs, the iron oxide content was set to identical values of corresponding NV solutions. Thus, when an NP dose is written as 1 $ng{\cdot}mL^{-1}$, the solution contains the same amount of Fe_2O_3 as an NV solution with 1 $ng{\cdot}mL^{-1}$ of grafted TRAIL.

Tumor necrosis factor-related apoptosis-inducing ligand-functionalized nanoparticles induce colon cancer cell death

The comparison of the effects of equimolar concentrations of TRAIL and NV on the viability of colon cancer cell line HCT116 was achieved, thanks to methylene blue staining, an assay that takes advantage of the loss of cell adherence, when cells die by apoptosis. Briefly, after stimulation, nonadherent, dying cells are removed by successive washes in phosphate buffered saline (PBS), and remaining cells are stained by methylene blue after fixation with methanol, allowing quantification of adherent surviving cells, shown here as % viability.

Figure 4A clearly illustrates the gain of function associated with TRAIL grafting onto NPs. NPs alone, irrespective of their size, even at high iron oxide concentrations, do not exhibit toxicity towards HCT116 cells. NV10 and NV100, on the other hand, were found to be more potent than TRAIL, with NV100 consistently displaying stronger activity than NV10.

Extrapolation of the IC_{50} of each compound from the experimental data gave values of 1.5 and 5 $ng{\cdot}mL^{-1}$ for NV100 and NV10, respectively, while that TRAIL was closer to 25 $ng{\cdot}mL^{-1}$. In agreement with this finding, NV100 was more potent than NV10 or TRAIL in inducing apoptosis in HCT116 cells, as demonstrated by nuclear fragmentation and annexin V staining (Fig. 4B and C). Whereas TRAIL induced apoptosis (annexin V/propidium iodide positivity) in approximately 50% of HCT116 cells, NV10 and NV100 induced apoptosis in more than 70% and 84% of the cells, respectively (Fig. 4C). Like TRAIL, albeit to a higher extend, NV10 and NV100 were found to induce postapoptotic necrosis (Garcia-Belinchon et al., 2015; Rogers et al., 2017). Importantly, however, NPs at the corresponding iron oxide concentrations were unable to trigger apoptosis in these cells (NP10: 8.9%; NP100: 13%; and control not stimulated (CTL): 9.7%). These results demonstrate that NV10 and NV100 are fivefold and 17-fold more potent, respectively, than TRAIL, which is consistent with previous results for TRAIL grafted onto carbon nanotubes (Zakaria et al., 2015).

Moreover, the specificity and the selectivity of NVs were assessed in HCT116 cells deficient for DR4 and DR5 (Dufour et al., 2017) (HCT116–DKO). In agreement with their selectivity towards TRAIL signaling and their lack of toxicity, neither NV10 nor NV100, even at high concentration (10 $\mu g{\cdot}mL^{-1}$), inhibited the viability of HCT116–DKO cells (Fig. 5).

A further demonstration of the superiority of NV100 is the finding that in parent HCT116 cells, 4 h after incubation, NV100 induced better activation of the TRAIL proapoptotic signaling pathway than NV10 or TRAIL, as assessed by immunoblotting (Fig. 6A). Likewise, although TRAIL signaling was moderately activated by TRAIL and NV10, a strong response was induced by NV100, as evidenced by the appearance of caspase-8 cleaved products p12 and p18, as well as downstream substrates, including caspase-3, lamin A and C, or PARP (Fig. 6A). In line with these findings, magnetic pull-down after NV10 or NV100 short incubations revealed the presence of TRAIL agonist receptors, namely, DR4 and DR5, as well as their death-induced signaling complex (DISC) components, FADD, caspase-8, and caspase-10, as soon as 5 min after stimulation (Fig. 6B). It should be stressed here that magnetic pull-down was performed in the absence of antibodies, allowing simultaneous detection of caspase-8 and caspase-10 in the same complex, which is usually not possible when immunocomplexes are pulled down using monoclonal antibodies, because of the cross-reactivity of secondary antibodies (Constantinescu et al., 2017). Remarkably, NV100 engaged TRAIL DISC very efficiently, allowing not only the pull-down of greater quantities of both FADD and DR5, in a time-dependent manner at 37°C, as compared with NV10 or TRAIL, but also induced better activation of both caspase-8 and caspase-10 within the DISC, as evidenced by the appearance of their cleaved products 30 min after stimulation (Fig. 6B).

Tumor necrosis factor-related apoptosis-inducing ligand-functionalized nanoparticles induce liver cancer cell death

Like the colon carcinoma cell line HCT116, human hepatocellular carcinoma cells (HepG2) express TRAIL agonist receptors but harbor in addition an antagonist

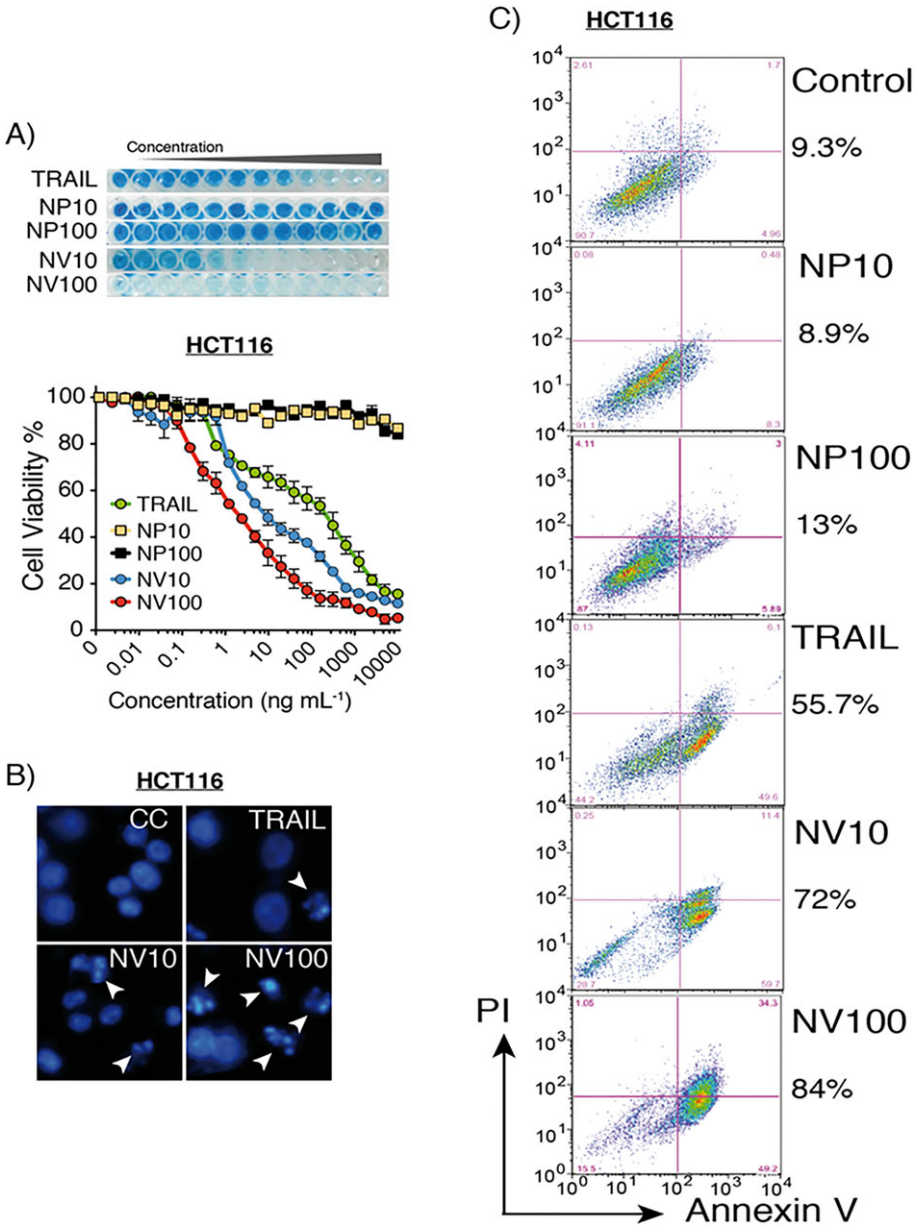

Figure 4. Cell death induced by of tumor necrosis factor-related apoptosis-inducing ligand (TRAIL), nanoparticles (NPs), and nanovectors (NVs) in HCT116 cells. (A) Methylene blue staining was used to measure cell viability of HCT116 cells stimulated with increasing concentrations of indicated compounds. Data are the mean ± standard deviation ($n = 3$). $^{*}p < 0.05$. (B) Hoechst staining of HCT116 treated with a fixed concentration (200 ng mL^{-1}) of TRAIL, NPs, and NVs for 16 h. (C) Apoptosis and necrosis were determined by annexin V and 7-AAD staining after stimulation earlier. The indicated percent represents cells positive for both markers and was calculated by FlowJo software after flow cytometry. PI, propidium iodide.

receptor, TRAIL-R4, that is known to confer resistance to TRAIL-induced apoptosis in these cells (Merino et al., 2006). Therefore, we next tried to find out whether TRAIL-functionalized NPs, NV10 and NV100, could overcome this resistance. HepG2 cells were incubated with NPs, NVs, or TRAIL for 16 h, and their viability was evaluated by resazurin assay. Despite the fact that this cell line is much less sensitive than the HCT116 colon cell line to TRAIL-induced cell death, because of the presence of TRAIL-R4 (Merino et al., 2006), NVs inhibited their viability by 50% at concentrations ranging from 10 to 50 ng·mL^{-1}, while TRAIL concentrations for similar effects were 20 to 100 times higher, reaching 1000 ng·mL^{-1} (Fig. 7A). At 200 ng·mL^{-1} TRAIL concentration, NV10 and NV100 killed more HepG2 cells than TRAIL, as evidenced by a live/dead cell staining assay (viable cells in green and dead cells in red) (Fig. 7B).

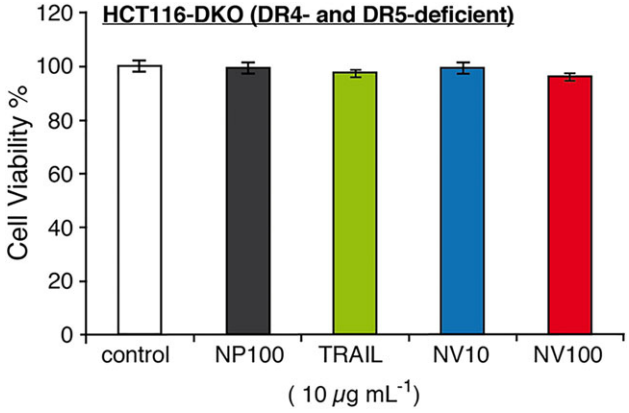

Figure 5. Cell viability of HCT116-DKO cells incubated with a high dose (10 μg·mL^{-1}) of free tumor necrosis factor-related apoptosis-inducing ligand (TRAIL), nanoparticles (NPs), or nanovectors (NVs). Viability was measured by methylene blue staining. Data are the mean ± standard deviation (n = 3).

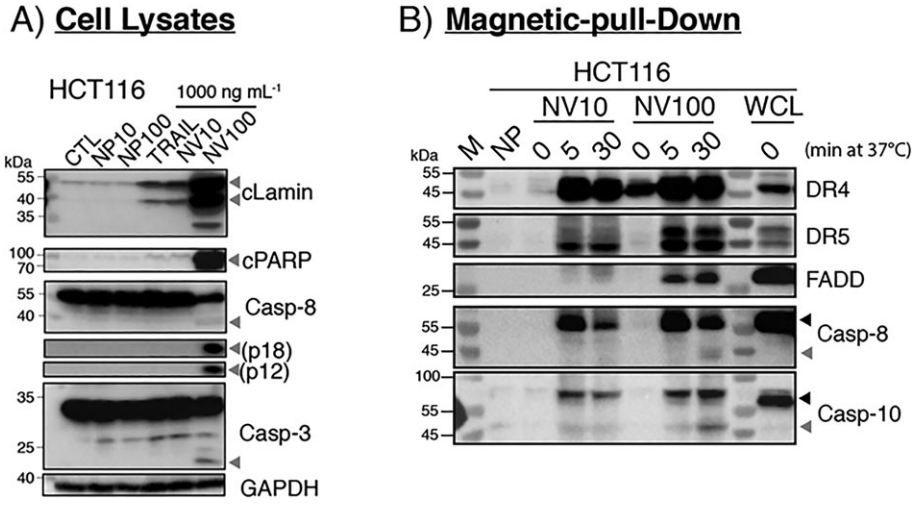

Figure 6. (A) Immunoblot analysis of HCT116-WT cells stimulated by tumor necrosis factor-related apoptosis-inducing ligand (TRAIL), nanoparticles (NPs), and nanovectors (NVs) (1 μg·mL^{-1}). Cleaved lamin, PARP, and caspase-8 (Casp-8) and caspase-3 (Casp-3) shown by grey arrows. (B) Magnetic pull-down of TRAIL death-induced signaling complex components in cells incubated for 5 or 30 min with TRAIL, NPs and NVs (2 ng·mL^{-1}). After cell lysis in buffer solution, the death-induced signaling complex was immunoprecipitated using a magnet, and associated proteins were analyzed by Western blotting using antibodies to DR4, DR5, FADD, caspase-8 (Casp-8), and caspase-10 (Casp-10). Molecular weights in kilodaltons. WCL, whole-cell lysates. Caspase proforms indicated by black arrows. Caspase-cleaved products shown by grey arrows.

Because concerns have been raised about the cytotoxicity of TRAIL on normal hepatocytes (Lawrence et al., 2001), we next evaluated the effects of NV10 and NV100 on primary rat hepatocytes. Fresh hepatocytes were isolated from healthy rats and stimulated for 24 h with high concentrations (10 μg·mL^{-1}) of TRAIL, NPs, and NVs, under the same conditions as those used for HepG2 cells, using resazurin assay. In contrast to HepG2 cells, treatment with NVs or TRAIL failed to induce cell death in healthy primary hepatocytes (Fig. 8A).

Live/dead stain assay on freshly isolated hepatocytes treated with TRAIL or NVs under the same conditions indicated that neither induces death in these cells (Fig. 8B). Moreover, markers associated with normal epithelial phenotypes (Haque et al., 2016), including albumin and E-cadherin, as assessed by immunofluorescence, confirmed that the strong expression of these markers, which are associated with healthy primary hepatocytes, was not altered in these cells after stimulation, confirming that TRAIL and TRAIL-derived NVs are harmless towards normal liver cells

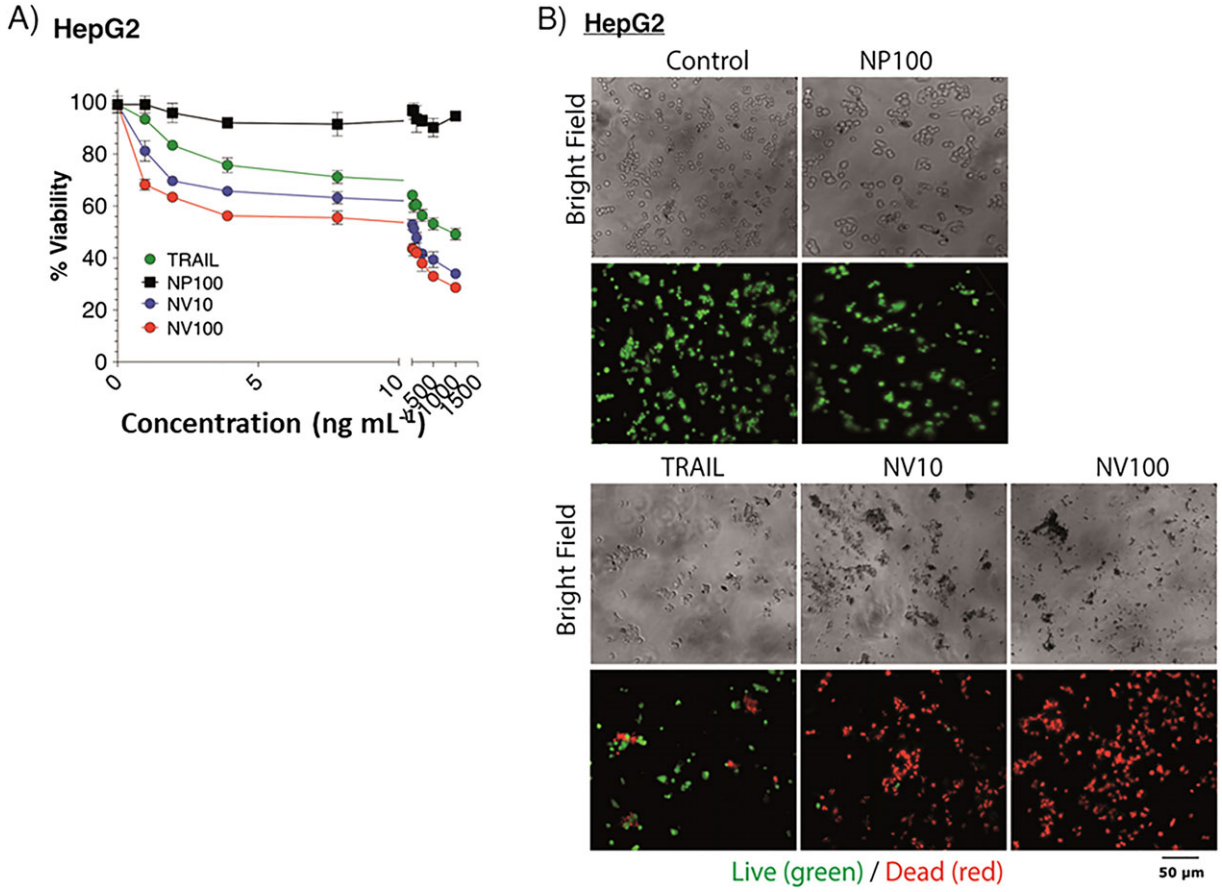

Figure 7. Effect of varying concentration of tumor necrosis factor-related apoptosis-inducing ligand (TRAIL) and nanovectors (NVs) on viability of HepG2 cells. (A) Cell viability was measured by resazurin assay. Fitted curves correspond to three independent experiments. (B) Brightfield microscopy (top panel) and live/dead cell staining showing the effect of TRAIL (200 ng·mL^{-1}) and NV treatment on the viability of HepG2 cells cultured for 6 h in the presence and absence of TRAIL. Untreated HepG2 cells cultured under the same conditions were used as control.

(Fig. 8C). DMSO was used here as a positive control for loss of hepatocyte viability. Our data provide evidence that TRAIL-functionalized NPs are both selective for cancer cells and safe for normal healthy cells.

Discussion

Tumor necrosis factor-related apoptosis-inducing ligand is a particularly promising antitumoral agent. Through its binding to its cognate agonistic receptors, namely, DR4 and DR5, TRAIL is able to induce apoptosis in malignant cells without harming healthy cells. Our findings are in line with other reports that combination of TRAIL as a recombinant protein (De Miguel et al., 2015a; De Miguel et al., 2015b; Kim et al., 2011a; Lim et al., 2011; Kim et al., 2011b; Kim et al., 2012; Guo et al., 2011a; Guo et al., 2011b; Guo et al., 2012; Muller et al., 2010) and a cDNA-encoding TRAIL (Miao et al., 2013; Sun et al., 2012) with a large variety of carrier NPs improves its therapeutic potential. Preliminary in vivo results on the use of such hybrids are very encouraging, although the drug was always injected into the tumors directly (Perlstein et al., 2013; Miao et al., 2013; Riehle et al., 2013) and not intravenously. The gain of function afforded by these formulations is thought to be due to increased solubilization and stability of the recombinant TRAIL in biological fluids (Lim et al., 2011; Muller et al., 2010; Na et al., 2008; Min et al., 2015), as well as to increased TRAIL valency (Pavet et al., 2010; Seifert et al., 2014a; Zakaria et al., 2015). The size of NPs has, so far, never been considered an issue, but our results provide evidence that it is likely to be important. TRAIL was coupled to crystallized 10- and 100-nm iron oxide NPs using a strong covalent peptide bond between the carboxylic and the amine groups of the former and the latter, respectively (section). The NP10 and NP100 iron oxide

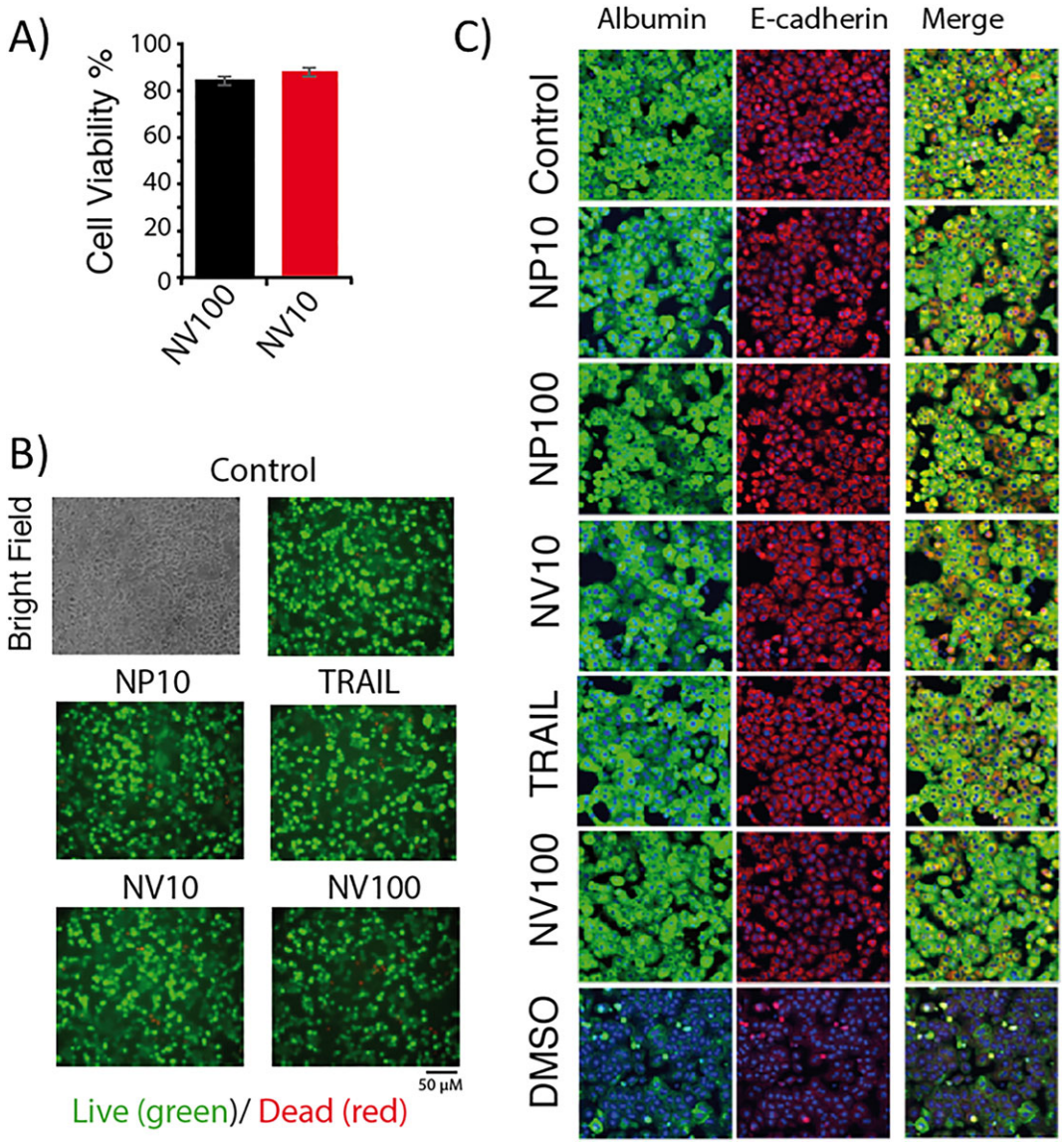

Figure 8. Effect of nanovectors (NVs) on the viability and epithelial phenotype of primary rat hepatocyte cells. Primary hepatocytes were cultured for 24 h on collage type I before treatment with 10 $\mu g \cdot mL^{-1}$ of tumor necrosis factor-related apoptosis-inducing ligand (TRAIL), nanoparticles (NPs), or NVs for 24 h. (A) No significant difference in cell viability was observed between hepatocytes with NVs versus control (not treated with NVs), as gauged by resazurin assay. Data are the mean ± standard deviation (n = 3). (B) Live/dead cell staining confirms the absence of any toxic effect from TRAIL and NVs. Untreated cells, cultured under the same conditions, were used as control. (C) Immunofluorescence staining of healthy epithelial (or hepatic) cell markers, albumin (green), and E-cadherin (cytoplasmic domain, red). Primary hepatocytes treated with 50% DMSO for 30 min were used as negative control.

cores do not trigger apoptosis, but both NVs exhibit greater proapoptotic activity in HCT116 and HepG2 cells than TRAIL. NV100 displays higher proapoptotic potential than NV10 on both tested tumor cell lines. It remains to be determined whether this higher activity of NV100 is related to its average core size (100 vs. 10 nm) or to the concentration of TRAIL grafted (about 8000 vs. 10 mol per particle). Analysis of TRAIL DISC formation, taking advantage of the magnetic properties of these NVs, demonstrates that TRAIL DISC components are more easily pulled down by NV100 than NV10, at equivalent TRAIL concentration. Like the soluble recombinant TRAIL protein, neither NV10 nor NV100 exhibits cytotoxicity towards normal hepatocytes or TRAIL receptor-deficient tumor cells (HCT116–DKO), indicating that these NVs induce death selectively

through TRAIL agonist receptors. We cannot exclude the possibility, though, that the different behaviors of NV10 and NV100 and thus their apoptotic potential might be governed by their different interactions with the cell surface because of their size. For instance, it is not clear whether these NVs accumulate on the cell surface or whether they are partly or totally internalized into the cytoplasm. One may hypothesize that NV10 due to its small size, like TRAIL itself, is internalized, while NV100 due to its large size remains on the cell membrane, making it able to pull down more TRAIL DISC components than NV10 or TRAIL. To date, whereas Perlstein et al. (2013) suggested that TRAIL-based hybrids obtained by coupling TRAIL to 70-nm iron oxide NPs could be internalized by glioma cells, Zakaria et al. (2015) found on the contrary that TRAIL–NCT hybrids on different hepatocarcinoma cell lines would not undergo internalization. Irrespective of their size, interaction with the cell surface or concentration of both NVs display greater activity than TRAIL towards cancer cells.

Altogether, albeit the molecular explanation for the gain of function described here still remains unclear, it can be proposed that these TRAIL-functionalized NPs, owing to the fact that they increase the TRAIL concentration locally onto a rigid platform, mimic naturally occurring membrane TRAIL, as NVs display a stronger ability to aggregate TRAIL receptors at the cell surface, allowing DISC formation, caspase-8 recruitment, and caspase activation (Fig. 9).

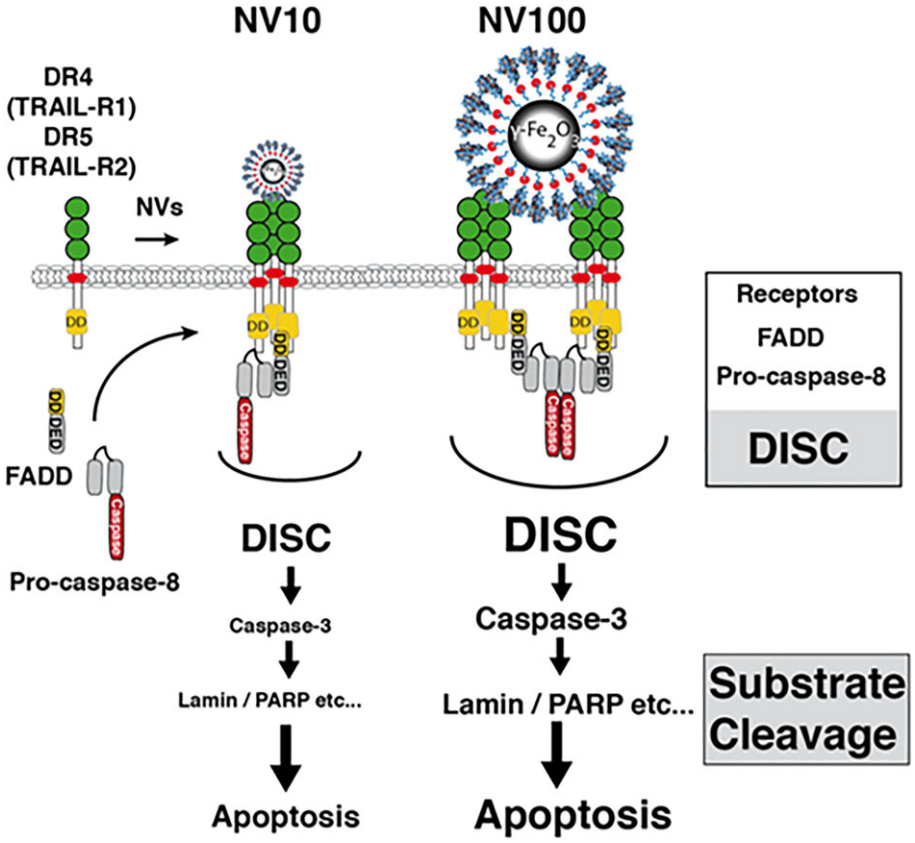

Figure 9. The extrinsic pathway is activated by extracellular ligands binding to cell-surface death receptors, which leads to the formation of the death-inducing signaling complex (DISC). Tumor necrosis factor-related apoptosis-inducing ligand (TRAIL) of nanovectors (NVs) binds to either TRAIL-R1 or TRAIL-R2 and induces their aggregation, enabling recruitment of the adaptor protein FADD, which in turn recruits the initiator caspases, pro-caspase-8 and/or caspase-10. Recruitment of the latter within the membrane constitutes the DISC, within which the proteases are activated. Active caspase-8 and caspase-10 are then released to the cytosol where they process pro-caspase-3, lamin, and PARP, among others. Activation of these effector caspases by proteolytic cleavage enables apoptosis. When caspase-8 and caspase-10 are not efficiently activated within the DISC, an amplification loop can supply sufficient effector caspase activation to engage the proapoptotic machinery. This backup signaling pathway proceeds via mitochondria and is initiated by caspase-8/caspase-10 through the cleavage of Bid.

Besides, it will be interesting to determine if these NVs, the smaller and the largest, can be combined to alternating current (AC) magnetic fields for MRI and/or therapeutic magnetic hyperthermia and particularly if their corresponding iron oxide doses are high enough to induce a significant magnetic response for such biophysical experiments. As a first answer, one can compare the NV10 and NV100 IC_{50} doses expressed as iron concentrations in $mg{\cdot}mL^{-1}$ (namely, 1.24 and 0.67 $mg{\cdot}mL^{-1}$ for HCT116 cells and 15.5 and 6.68 $mg{\cdot}mL^{-1}$ for HepG2 cells) with those clinically used for iron oxide-based MRI contrasting. As an example, the recommended dosage of RESOVIST, one of the most popular iron oxide-based MRI contrast agents and sold as injectable 28 $mg{\cdot}mL^{-1}$ solution of iron, is 0.9 and 1.4 mL for adult patients of less and more than 60 kg, respectively (Wang and Ng, 2011). These doses are comparable with the IC_{50}s of the NVs. As a second answer, one has to check the ability of the engineered NPs to generate heat when an external AC magnetic field is applied and to induce cell death. We have already established the magnetocalorimetric properties of coated (Hai et al., 2017) and uncoated (Hanini et al., 2016) polyol-made iron oxide NPs and their ability to induce malignant cell apoptosis by hyperthermia, opening up synergetic therapeutic opportunities. Indeed, a local rise of temperature under an applied AC magnetic field can sensitize tumor cells to TRAIL-induced apoptosis (Morle et al., 2015; Moulin and Arrigo, 2008; Moulin et al., 2007; Yoo et al., 2006) as it can compensate the lack of efficiency of TRAIL in certain resistant cells (Song et al., 2012).

Experimental

Nanovector production

NP10 and NP100 synthesis

Iron oxide NPs of two different diameters, 10 and 100 nm (Fig. 10), were prepared by the polyol method (Basti et al., 2010; Hanini et al., 2016), the size and shape being controlled by adjusting the amount of distilled water added (0.110 and 0.025 mol, respectively) and the nature of the iron salt (acetate and lactate,

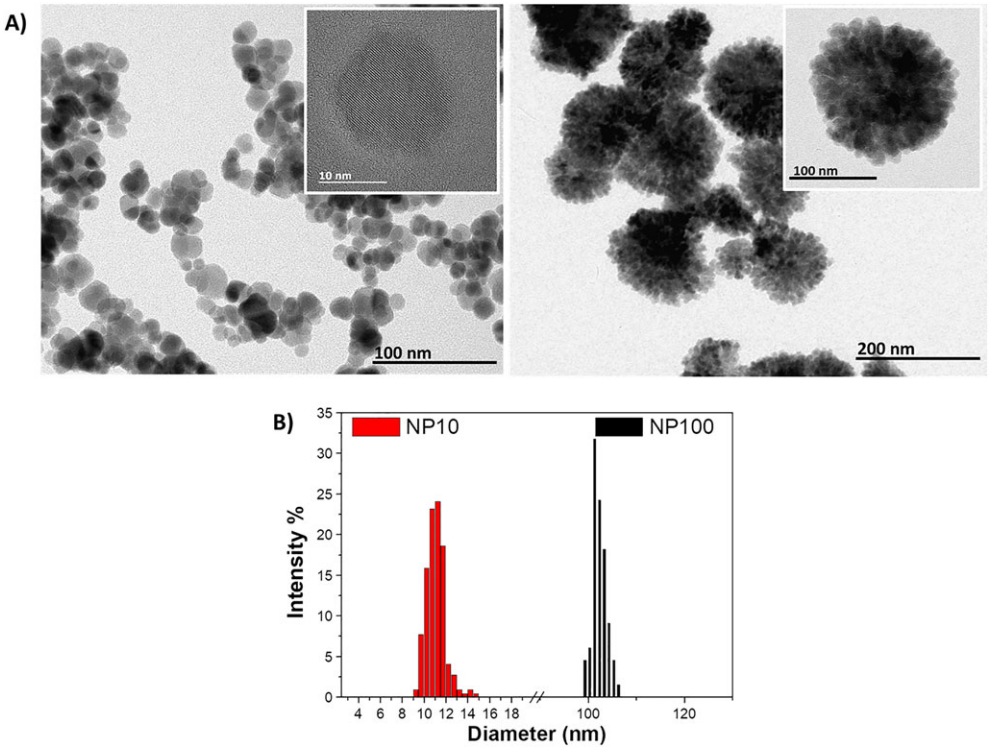

Figure 10. (A) Transmission electron microscopy (TEM) images of an assembly of 10- and 100-nm iron oxide nanoparticles (NPs), recorded on a JEOL II microscope, operating at 100 kV. High-resolution TEM micrographs (inset) illustrate the single crystal type of the smaller NPs and the polycrystal type of the larger ones. (B) Size distribution of particles as inferred from statistical analysis of TEM micrographs using ImageJ software and assuming a spherical shape. The average diameter and the standard deviation were deduced from a log-normal fitting.

respectively). The metallic salt and the water were added to 250 mL of diethylene glycol. The mixture was refluxed, and the temperature was increased at a rate of 6°C·min^{-1} with mechanical stirring up to the boiling point (230°C) and maintained at this temperature for 3 h. The mixture was then cooled to room temperature.

Tumor necrosis factor-related apoptosis-inducing ligand grafting

Nanoparticles were first functionalized by APTES (Fig. 11A) Piraux et al., 2013. In practice, 100 mg of fresh NPs was dispersed by ultrasonication in 10 mL of methanol, and 250 mL of ethanol was added to the dispersion. One milliliter of APTES was added slowly to the earlier mixture, which was ultrasonicated for 1 h. The mixture was boiled under argon for 2 h to react APTES with the NP surface hydroxyl groups. It was then cooled to room temperature, and the NP-APTES were washed at least four times with ethanol, collected by sedimentation on a laboratory magnet, and dried in air. They were finally coupled to TRAIL using the well-known NHS-EDC route. *N*-Hydroxysuccinimide (NHS) and 1-ethyl-3-(3 dimethylaminopropyl)carbodiimide (EDC) were added to TRAIL solution (1 mg·mL^{-1}) to achieve final concentrations of 3.75 and 1.50 mM, respectively (Fig. 11B). Five milligrams of NP-APTES were then introduced into

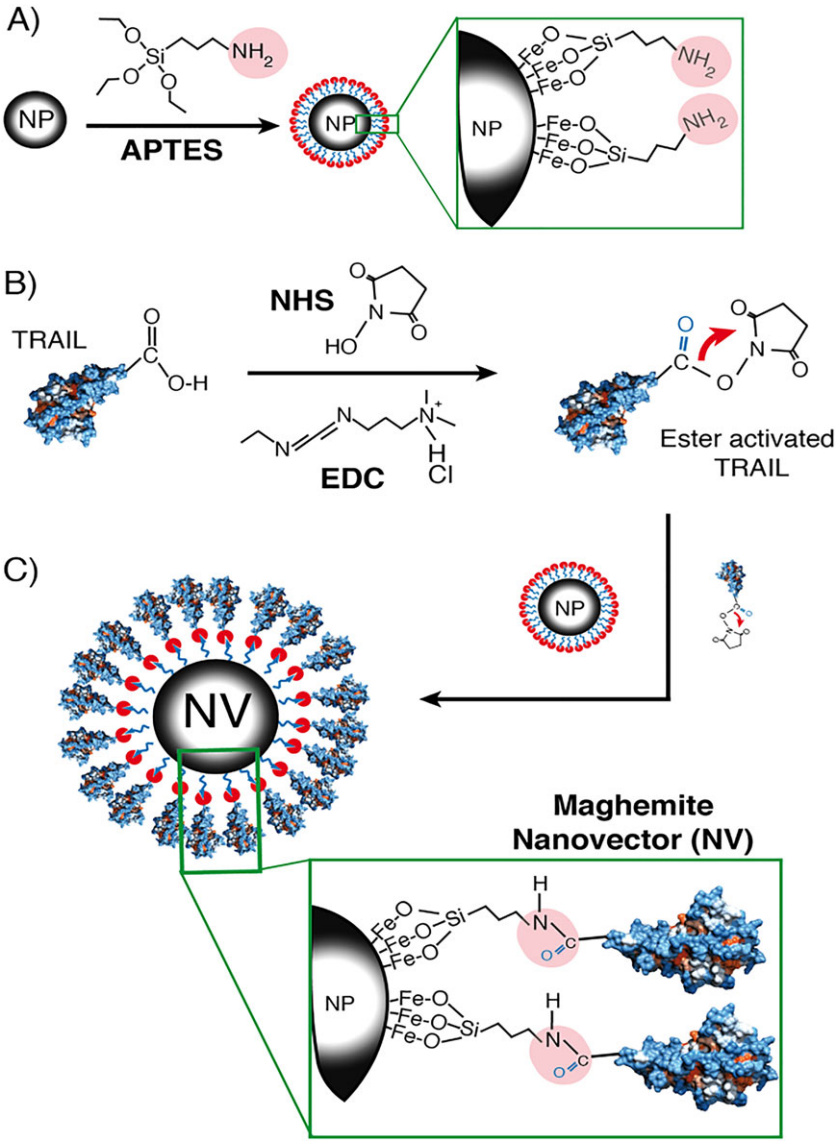

Figure 11. Schematic illustration of (A) the amination of the nanoparticle (NP) surface by APTES, (B) the activation of the carboxylate groups of tumor necrosis factor-related apoptosis-inducing ligand (TRAIL) by EDC-NHS, and (C) the TRAIL-NP coupling.

the reaction solution. The resulting suspension was stirred at 4°C overnight after the addition of 1 mL of PBS buffer at pH 9. Under these conditions, amide bonds are formed between the NP-APTES surface amino groups and the activated peripheral TRAIL carboxylic groups (Fig. 11C).

The hybrid NVs formed were finally washed several times with PBS buffer and recovered by magnetic decantation.

The grafting was rapidly checked by comparing the FTIR spectra (not shown) of the NVs with those of pristine NPs, using the KBr method on a Nicolet Magna-IR 860 spectrophotometer. The signature of amide groups is clearly evidenced in the 1650-1550 cm^{-1} spectral range.

Nanovector characterization

Surface charge

To determine the surface charge of the as-produced NPs and NVs, their ζ potential (Fig. 12) was measured at room temperature starting from their aqueous solution (1 $g{\cdot}L^{-1}$) and varying their pH, using a Malvern Nano Zetasizer, after vigorous sonication for 10 min. Interestingly, whatever the magnetic core size, NPs and NVs exhibit an isoelectric point comprised between pH 6.5 and pH 7.0.

Tumor necrosis factor-related apoptosis-inducing ligand grafting quantification

The mean concentration of TRAIL grafted on NPs was estimated by different techniques. First, X-ray photoelectron spectroscopy was performed on dried NPs and NVs to assess the atomic N/Fe ratio, nitrogen being mainly introduced by TRAIL, while Fe comes from the iron oxide. The spectra were recorded on an ESCALAB 250 (Thermo VG Scientific) machine, equipped with a monochromatic Al Kα X-ray source (1486.6 eV). All the analyses were performed by fixing the incident X-ray spot size to 650 μm on the sampling holder and the pass energy to 100 and 40 eV for the survey and high-resolution measurement modes, respectively. Spectral calibration was determined by setting the main C (1s) component to 285 eV. Second, routine magnetometry was carried out on a Quantum Design MPMS-XL SQUID magnetometer, and virgin magnetization curves were recorded at 5 K on all the samples, attributing the saturation magnetization decrease of NVs to their diamagnetic TRAIL content. Third, thermogravimetry analyses were conducted in air on a Labsys-Evo equipment with a heating rate of 10°C·min^{-1}, up to 800°C, the observed weight losses on NVs being mainly attributed to TRAIL departure. Finally, the conventional protein titration Bradford method (Bradford, 1976) was used to estimate the amount of grafted TRAIL. It consists of (1) measuring the TRAIL absorbance in the supernatant of the grafting solution (plus the washing solutions) after magnetic decantation; (2) calculating its corresponding concentration, thanks to a calibration curve; and then (3) subtracting the estimated value from the nominal one.

Biological assays

Cell lines and cell culture

Human colon adenocarcinoma cell line HCT116 (CCL-247™) was purchased from ATCC® (Manassas, VA, USA) and grown in 10% fetal calf serum (FCS)-supplemented Dulbecco's modified Eagle's medium (DMEM) containing 4.5% glucose and 2 mM glutamine. Adherent cells were seeded at 30% confluence (approx. 80,000 cells per cm^2). Pharmacological modulation was

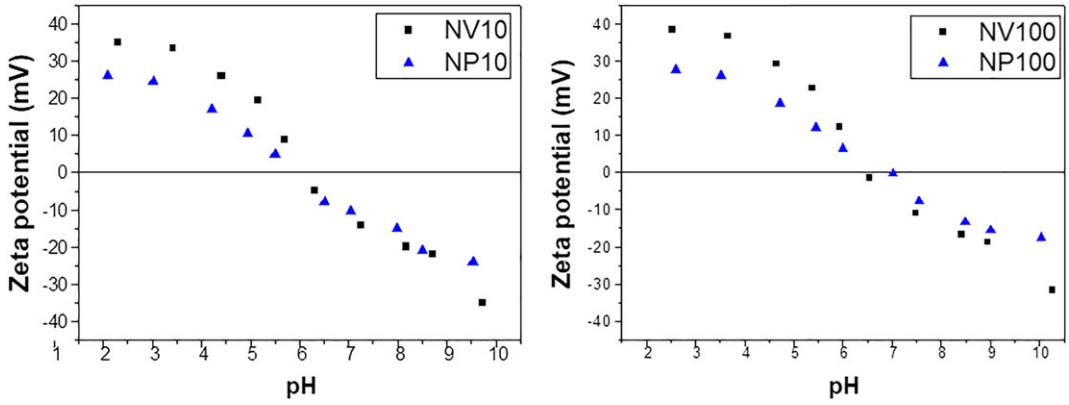

Figure 12. Zeta potential measured as a function of pH on aqueous suspension of pristine NP10/NP100 and their NV10/NV100 hybrids.

initiated at 60–70% confluence. Cells were recovered after stimulation by trypsinization and centrifugation at 500 *g* for 3 min at 4°C.

Tumor necrosis factor-related apoptosis-inducing ligand receptor-deficient HCT116 (DKO) cells were generated by the TALEN approach, described by Dufour et al. (2017).

Human hepatocellular carcinoma cell line, HepG2, was purchased from American Type Culture Collection. HepG2 cells were cultured in 50% Ham's F-12 medium (BioWhittaker Co.) and 50% DMEM (Gibco, 11995), supplemented with 5% (v/v) FCS (Invitrogen) and 1% (v/v) penicillin–streptomycin.

Adult female Lewis rat-derived primary hepatocytes (Charles River Laboratories, Boston, MA, USA) were maintained according to the protocol published elsewhere Haque et al., 2016. Briefly, rat liver tissue was digested with EDTA and collagenase IV solution followed by purification by Percoll density gradient centrifugation. Primary hepatocytes were maintained in DMEM supplemented with 10% (v/v) FBS, 0.5 $U \cdot mL^{-1}$ insulin (Novolin N), 20 $ng \cdot mL^{-1}$ epidermal growth factors (Invitrogen), 7 $ng \cdot mL^{-1}$ glucagon (Sigma), 7.5 $\mu g \cdot mL^{-1}$ hydrocortisone sodium succinate (Pfizer), and 1% (v/v) penicillin–streptomycin. All cell lines were grown at 37°C in a humidified 5% CO_2 atmosphere. Media were changed every 2 days.

Cell viability and apoptosis assays

Viability of HCT116 was assessed by methylene blue assay. The 5×10^4 cells were seeded per well (0.32 cm^2) in 96-well plates and incubated as earlier with his-TRAIL and/or NVs NV10/NV100 from (0 to 104 $ng \cdot mL^{-1}$). After 16 h, cells were washed in PBS buffer solution and fixed by 2% paraformaldehyde for 20 min at room temperature, washed three times in PBS, and stained by 5% methylene blue for 30 min. After three subsequent gentle washes in PBS, methylene blue was eluted in 1% HCl for 4 h at ambient temperature. Optical density was then measured at 630 nm.

Cell viability of primary hepatocytes was assessed by resazurin assay. In 24-well plates, 10^5 cells of were plated in the presence of his-hTRAIL and/or NV10/NV100 at a concentration as high as 10^4 $ng \cdot mL^{-1}$. Optical density was measured at 563 nm. HepG2 cells and primary hepatocyte samples for live/dead cell analysis were stained using manufacturer's instructions (Live/Dead Cell Viability Kit, Life Technologies). Briefly, cells were washed with PBS prior to the treatment with PBS containing 4 μM ethidium homodimer and 2 μM calcein AM for 30 min at 37°C. The samples were then rinsed with fresh PBS before being imaged by a laser-scanning confocal microscope (LSM700, Carl Zeiss, Jena, Germany). Apoptosis of HCT116 was determined by detection of phosphatidylserine externalization after colabeling with annexin 5 (a5)-FITC/7AAD. Fluorescence acquisition of a5/7AAD was performed using flow cytometry (BD FACSCanto™ 10 platform). Apoptosis was expressed as the percentage of cells presenting positive labeling versus negative-labeled counterparts (viable cells: a5− and 7AAD−; early apoptosis: a5+ and 7AAD−; late apoptosis/necrosis a5+ and 7AAD+; and debris: a5− and 7AAD+, etc.). Each statistical analysis relied on a minimum of 10,000 events.

Apoptosis was confirmed by nuclear fragmentation assay using Hoechst staining. The 5×10^5 cells were stimulating by 200 $ng \cdot mL^{-1}$ of his-TRAIL and/or NV10/NV100 for 8 h. Cells were then incubated for 15 min in a cell disaggregation and counting solution (Accumax: Interchim, Montluçon, France)/PBS. Fixation was achieved by overnight incubation in the dark, at 4°C in a 200 μL solution containing: PBS + 1% paraformaldehyde + 1 mM Hoechst, and followed by subsequent washes. Image acquisition was performed using an inverted fluorescence microscope (Leica DMIRB platform) connected to an Axiocam device. Pictures were analyzed by AXIO-Vs 40 V 4.8.2.0 Carl Zeiss MicroImagin software.

Immunofluorescence imaging

Primary hepatocytes cultured for 24 h in 24-well plates were washed with PBS in order to remove the media prior to the fixation step. Cells were fixed in 4% paraformaldehyde + 0.2% Triton-X100 in PBS for 15 min. The cells were then washed three times with PBS and incubated in blocking solution (1% bovine serum albumin in PBS) for 60 min. The samples were then incubated with primary antibodies for 90 min at room temperature and washed three times to remove unbound antibodies. Finally, the samples were incubated with a mixture of secondary antibodies and DAPI (Invitrogen) for 60 min and washed with PBS three times before images were taken. All experiments were carried out at room temperature. The primary antibodies used were sheep anti-rat albumin (1:100; Bethyl Laboratories Inc.) and mouse anti-E-cadherin (1:50; BD Transduction Laboratories). The secondary antibodies used were Alexa-488 donkey anti-sheep IgG and Alexa-546 donkey anti-mouse IgG. Stained

cells were visualized and imaged using a laser-scanning confocal microscope.

Immunoprecipitation

For DISC analysis, 50 × 106 cells were stimulated by 200 ng·mL^{-1} of NVs in 10 mL of complete medium, for the indicated times at 37°C. Cells were then centrifuged at 400 *g* for 5 min at 4°C, washed with PBS, and then lysed in 1 mL lysis buffer containing 1% NP40 (Nonidet P40, Sigma-Aldrich), 20 mM of Tris-HCl (pH 7.5), 150 mM of NaCl, and 10% of glycerol, in the presence of a protease inhibitor cocktail (pepstatin A, 2.5 mg·mL^{-1}; aprotinin, 10 mg·mL^{-1}; trypsin inhibitor, 2.5 mg·mL^{-1}; and leupeptin, 5 mg·mL^{-1}; Roche, France) and of 5 μM of Z-vad. Insoluble fragments were pulled down by a magnet several times until a clear lysate was obtained. One hundred microliters of loading buffer containing 10% DTT was added to samples that were further denaturated for 5 min at 95°C for immunoblot. For DISC analysis, 5 × 10^7 cells were treated by 2 μg·mL^{-1} of NV10/NV100 in suspension in 5 mL FCS-enriched medium, for the indicated periods at 37°C. After stimulation, cell response was stopped on ice for 15 min. Cells were then centrifuged at 500 *g* for 3 min at 4°C, washed three times with PBS, and then lysed in 1 mL lysis buffer containing 1% NP40 (Nonidet P40, Sigma-Aldrich), 20 mM of Tris-HCl (pH 7.5), 150 mM of NaCl, and 10% of glycerol, in the presence of a protease inhibitor cocktail. When indicated, 5 μM of Z-vad was added to the solution. Insoluble fragments were pulled down and removed by a magnet several times until a clear lysate was obtained. One hundred microliters of loading buffer containing 10% DTT was added to samples that were further denaturized for 5 min at 95°C before immunoblotting.

Western blotting

Immunoprecipitates were resolved by 12% sodium dodecyl sulfate-polyacrylamide gel electrophoresis and transferred to nitrocellulose (Bio-Rad) membranes. Nonspecific binding sites were blocked by incubation in PBS containing 0.5% Tween 20 and 5% milk, for 1 h at room temperature. Immunoblots were then incubated overnight with the following specific primary antibodies: FLIPL (Adipogen), FADD (BD Transduction Laboratories), caspase-8 or 10 (MBL), and DR4 and DR5 (Merck Millipore). Thereafter, three washes were performed in PBS containing 0.5% Tween 20 followed by incubation with horseradish peroxidase-conjugated secondary antibody. The membranes were then revealed using enhanced chemiluminescence substrate (WesternBright Quantum Western blotting detection kit; Advansta). Immunoreactive bands were detected by the ChemiDoc platform (Bio-Rad), using an incremental imaging method. Results were analyzed by Image Lab software (Bio-Rad).

Conclusion

Coupling TRAIL to iron oxide NPs increases its apoptotic activity on HCT116 and HepG2 cells. For the first time, we demonstrate that the apoptotic potential of TRAIL-derivative depends drastically of the size the NPs to which it is functionalized. NV100 is being more potent than NV10 as illustrated by its greater ability to induce DISC formation, recruit caspase-8, and trigger apoptosis. Moreover, the magnetic properties of NV100 allow them to image drug delivery by MRI and to be manipulated by an external AC magnetic field. Therefore, the targeting capabilities of NV100 added to its potential use in magnetic hyperthermia (experiments are investigated in our future study) make this NV a good candidate for application in cancer therapy.

Acknowledgments

The ANR (Agence Nationale de la Recherche) and the CGI (Commissariat à l'Investissement d'Avenir) are gratefully acknowledged for their financial support of this study through the Labex LipSTIC (ANR-11-LABX-0021-01) and Labex SEAM (ANR 11 LABX 086 and ANR 11 IDEX 05 02). O. Micheau was also supported by the Fondation ARC.

The authors are grateful to Dr. Angelique Louis, from UC Davis, for hosting H. Belkahla in her group during several weeks and helping her in the achievement of several important in vitro and in vivo assays on the produced nanoparticles. They also want to thank Dr. John S. Lomas, from Paris Diderot University, for providing language help and English writing assistance.

Funding Information

The ANR (Agence Nationale de la Recherche) and the CGI (Commissariat à l'Investissement d'Avenir) are gratefully acknowledged for their financial support of this study through the Labex LipSTIC (ANR-11-LABX-0021-01) and Labex SEAM (ANR 11 LABX 086 and ANR 11 IDEX 05 02). O. Micheau was also supported by the Fondation ARC.

Conflict of Interest

None declared.

REFERENCES

Alexiou, C., Jurgons, R., Schmid, R., Hilpert, A., Bergemann, C., Parak, F., and Iro, H. **2005**. In vitro and in vivo investigations of targeted chemotherapy with magnetic nanoparticles. J Magn Magn Mater *293*:389–393.

Almasan, A., and Ashkenazi, A. **2003**. Apo2L/TRAIL: apoptosis signaling, biology, and potential for cancer therapy. Cytokine Growth Factor Rev. *14*:337–348.

Baird, R. D., and Kaye, S. B. **2003**. Drug resistance reversal – are we getting closer? Eur. J. Cancer *39*:2450–2461.

Basti, H., Ben Tahar, L., Smiri, L. S., Herbst, F., Vaulay, M. J., Chau, F., Ammar, S., and Benderbous, S. **2010**. Catechol derivatives-coated Fe_3O_4 and γ-Fe_2O_3 nanoparticles as potential MRI contrast agents. J Colloid Interf Sci *341*:248–254.

Bear, J. C., Patrick, P. S., Casson, A., Southern, P., Lin, F.-Y., Powell, M. J., Pankhurst, Q. A., Kalber, T., Lythgoe, M., Parkinand, I. P., and Mayes, A. G. **2016**. Magnetic hyperthermia controlled drug release in the GI tract: solving the problem of detection. Sci. Rep. *6*:34271.

Bharti, C., Nagaich, U., Pal, A. K., and Gulati, N. **2015**. Mesoporous silica nanoparticles in target drug delivery system: a review. Int J Pharm Investig *5*:124–133.

Bradford, M. M. **1976**. A rapid and sensitive method for the quantitation of microgram quantities of protein utilizing the principle of protein-dye binding. Anal. Biochem. *72*:248–254.

Constantinescu, A. A., Morle, A., and Micheau, O. **2017**. Immunoprecipitation of death inducing signaling complex by caspase-8. Methods Mol. Biol. *1557*:19–31.

De Miguel, D., Gallego-Lleyda, A., Anel, A., and Martinez-Lostao, L. **2015a**. Liposome-bound TRAIL induces superior DR5 clustering and enhanced DISC recruitment in histiocytic lymphoma U937 cells. Leuk. Res. *39*: 657–666.

De Miguel, D., Gallego-Lleyda, A., Galan-Malo, P., Rodriguez-Vigil, C., Marzo, I., Anel, A., and Martinez-Lostao, L. **2015b**. Immunotherapy with liposome-bound TRAIL overcomes partial protection to soluble TRAIL-induced apoptosis offered by down-regulation of Bim in leukemic cells. Clin. Transl. Oncol. *17*:657–667.

Douziech-Eyrolles, L., Marchais, H., Herve, K., Munnier, E., Souce, M., Linassier, C., Dubois, P., and Chourpa, I. **2007**. Nanovectors for anticancer agents based on superparamagnetic iron oxide nanoparticles. Int. J. Nanomedicine *2*:541–550.

Dufour, F., Rattier, T., Constantinescu, A. A., Zischler, L., Morle, A., Ben Mabrouk, H., Humblin, E., Jacquemin, G., Szegezdi, E., Delacote, F., Marrakchi, N., Guichard, G., Pellat-Deceunynck, C., Vacher, P., Legembre, P., Garrido, C., and Micheau, O. **2017**. TRAIL receptor gene editing unveils TRAIL-R1 as a master player of apoptosis induced by TRAIL and ER stress. Oncotarget *8*: 9974–9985.

Garcia-Belinchon, M., Sanchez-Osuna, M., Martinez-Escardo, L., Granados-Colomina, C., Pascual-Guiral, S., Iglesias-Guimarais, V., Casanelles, E., Ribas, J., and Yuste, V. J. **2015**. An early and robust activation of caspases heads cells for a regulated form of necrotic-like cell death. J. Biol. Chem. *290*:20841–20855.

Guo, L., Fan, L., Pang, Z., Ren, J., Ren, Y., Li, J., Chen, J., Wen, Z., and Jiang, X. **2011a**. TRAIL and doxorubicin combination enhances anti-glioblastoma effect based on passive tumor targeting of liposomes. J. Control. Release *154*:93–102.

Guo, L., Fan, L., Ren, J., Pang, Z., Ren, Y., Li, J., Wen, Z., and Jiang, X. **2011b**. A novel combination of TRAIL and doxorubicin enhances antitumor effect based on passive tumor-targeting of liposomes. Nanotechnology *22*:265105.

Guo, L., Fan, L., Ren, J., Pang, Z., Ren, Y., Li, J., Wen, Z., Qian, Y., Zhang, L., Ma, H., and Jiang, X. **2012**. Int. J. Nanomedicine *7*:1449–1460.

Hai, J., Piraux, H., Mazarío, E., Volatron, J., Ha-Duong, N. T., Decorse, P., Lomas, J. S., Verbeke, P., Ammar, S., Wilhelm, C., El Hage Chahine, J.-M., and Hemadi, M. **2017**. Maghemite nanoparticles coated with human serum albumin: combining targeting by the iron-acquisition pathway and potential in photothermal therapies. J. Mater. Chem. B *5*:3154–3162.

Hanini, A., Schmitt, A., Kacem, K., Chau, F., Ammar, S., and Gavard, J. **2011**. Int. J. Nanomedicine *6*:787–794.

Hanini, A., Lartigues, L., Gavard, J., Schmitt, A., Kacem, K., Wilhelm, C., Gazeau, F., Chau, F., and Ammar, S. **2016**. Thermosensitivity profile of malignant glioma U87-MG cells and human endothelial cells following γ-Fe_2O_3NPs internalization and magnetic field application. RSC Adv. *6*:15415–15423.

Haque, A., Gheibi, P., Gao, Y., Foster, E., Son, K. J., You, J., Stybayeva, G., Patel, D., and Revzin, A. **2016**. Cell biology is different in small volumes: endogenous signals shape phenotype of primary hepatocytes cultured in microfluidic channels. Sci. Rep. *6*:33980.

Holler, N., Kataoka, T., Bodmer, J. L., Romero, P., Romero, J., Deperthes, D., Engel, J., Tschopp, J., and Schneider, P. **2000**. Development of improved soluble inhibitors of FasL and CD40L based on oligomerized receptors. J. Immunol. Methods *237*:159–173.

Huang, Y.-J., and Hsu, S.-H. **2017**. TRAIL-functionalized gold nanoparticles selectively trigger apoptosis in polarized macrophages. Nanotheranostics *1*:326–337.

Jain, K. T., Richey, J., Strand, M., Leslie-Pelecky, D. L., Flask, C., and Labhasetwar, V. **2008**. Magnetic nanoparticles with dual functional properties: drug delivery and magnetic resonance imaging. Biomaterials *29*: 4012–4021.

Kim, T. H., Jiang, H. H., Youn, Y. S., Park, C. W., Lim, S. M., Jin, C. H., Tak, K. K., Lee, H. S., and Lee, K. C. **2011a**. Preparation and characterization of Apo2L/TNF-related apoptosis-inducing ligand-loaded human serum albumin nanoparticles with improved stability and tumor distribution. J Pharm Sci-Us *100*:482–491.

Kim, T. H., Jiang, H. H., Park, C. W., Youn, Y. S., Lee, S., Chen, X., and Lee, K. C. **2011b**. PEGylated TNF-related apoptosis-inducing ligand (TRAIL)-loaded sustained release PLGA microspheres for enhanced stability and antitumor activity. J. Control. Release *150*:63–69.

Kim, T. H., Jo, Y. G., Jiang, H. H., Lim, S. M., Youn, Y. S., Lee, S., Chen, X. Y., Byun, Y., and Lee, K. C. **2012**. PEG-transferrin conjugated TRAIL (TNF-related apoptosis-inducing ligand) for therapeutic tumor targeting. J. Control. Release *162*:422–428.

Kim, H., Jeong, D., Kang, H. E., Lee, K. C., and Na, K. **2013**. A sulfate polysaccharide/TNF-related apoptosis-inducing ligand (TRAIL) complex for the long-term delivery of TRAIL in poly(lactic-co-glycolic acid) (PLGA) microspheres. J. Pharm. Pharmacol. *65*:11–21.

Kreuter, J. **2004**. Encyclopedia. Nanosci Nanotechnol *7*:161–180.

Laurent, S., Dutz, S., Hafeli, U. O., and Mahmoudi, M. **2011**. Magnetic fluid hyperthermia: focus on superparamagnetic iron oxide nanoparticles. Adv Colloid Interfac *166*:8–23.

Lawrence, D., Shahrokh, Z., Marsters, S., Achilles, K., Shih, D., Mounho, B., Hillan, K., Totpal, K., DeForge, L., Schow, P., Hooley, J., Sherwood, S., Pai, R., Leung, S., Khan, L., Gliniak, B., Bussiere, J., Smith, C. A., Strom, S. S., Kelley, S., Fox, J. A., Thomas, D., and Ashkenazi, A. **2001**. Differential hepatocyte toxicity of recombinant Apo2L/TRAIL versions. Nat. Med. *7*: 383–385.

Lim, S. M., Kim, T. H., Jiang, H. H., Park, C. W., Lee, S., Chen, X., and Lee, K. C. **2011**. Improved biological half-life and anti-tumor activity of TNF-related apoptosis-inducing ligand (TRAIL) using PEG-exposed nanoparticles. Biomaterials *32*:3538–3546.

Merino, D., Lalaoui, N., Morizot, A., Schneider, P., Solary, E., and Micheau, O. **2006**. Differential inhibition of TRAIL-mediated DR5-DISC formation by Decoy receptors 1 and 2. Molr & Cell Biol *26*:7046–7055.

Merino, D., Lalaoui, N., Morizot, A., Solary, E., and Micheau, O. **2007**. TRAIL in cancer therapy: present and future challenges. Expert Opin. Ther. Targets *11*: 1299–1314.

Miao, L., Zhang, K., Qiao, C., Jin, X., Zheng, C., Yang, B., and Sun, H. **2013**. Antitumor effect of human TRAIL on adenoid cystic carcinoma using magnetic nanoparticle-mediated gene expression. Nanomedicine *9*:141–150.

Micheau, O., Shirley, S., and Dufour, F. **2013**. Death receptors as targets in cancer. Brit J Pharmacol *169*:1723–1744.

Min, S. Y., Byeon, H. J., Lee, C., Seo, J., Lee, E. S., Shin, B. S., Choi, H. G., Lee, K. C., and Youn, Y. S. **2015**. Facile one-pot formulation of TRAIL-embedded paclitaxel-bound albumin nanoparticles for the treatment of pancreatic cancer. Int. J. Pharm. *494*:506–515.

Morle, A., Garrido, C., and Micheau, O. **2015**. Hyperthermia restores apoptosis induced by death receptors through aggregation-induced c-FLIP cytosolic depletion. Cell Death Dis. *6*:e1633.

Moulin, M., and Arrigo, A. P. **2008**. Caspases activation in hyperthermia-induced stimulation of TRAIL apoptosis. Cell Stress Chaperones *13*:313–326.

Moulin, M., Dumontet, C., and Arrigo, A. P. **2007**. Sensitization of chronic lymphocytic leukemia cells to TRAIL-induced apoptosis by hyperthermia. Cancer Lett. *250*:117–127.

Muller, N., Schneider, B., Pfizenmaier, K., and Wajant, H. **2010**. Superior serum half life of albumin tagged TNF ligands. Biochem Bioph Res Co *396*:793–799.

Na, S. J., Chae, S. Y., Lee, S., Park, K., Kim, K., Park, J. H., Kwon, I. C., Jeong, S. Y., and Lee, K. C. **2008**. Stability and bioactivity of nanocomplex of TNF-related apoptosis-inducing ligand. Int. J. Pharm. *363*:149–154.

Pavet, V., Beyrath, J., Pardin, C., Morizot, A., Lechner, M.-C., Briand, J.-P., Wendland, M., Maison, W., Fournel, S., Micheau, O., Guichard, G., and Gronemeyer, H. **2010**. Multivalent DR5 peptides activate the TRAIL death pathway and exert tumoricidal activity. Cancer Res. *70*:1101–1110.

Perlstein, B., Finniss, S. A., Miller, C., Okhrimenko, H., Kazimirsky, G., Cazacu, S., Lee, H. K., Lemke, N., Brodie, S., Umansky, F., Rempel, S. A., Rosenblum, M., Mikklesen, T., Margel, S., and Brodie, C. **2013**. TRAIL conjugated to nanoparticles exhibits increased anti-tumor activities in glioma cells and glioma stem cells in vitro and in vivo. Neuro Oncol. *15*:29–40.

Piraux, H., Hai, J., Verbeke, P., Serradji, N., Ammar, S., Losno, R., Ha-Duong, N. T., Hemadi, M., and El Hage Chahine, J. M. **2013**. Transferrin receptor-1 iron-acquisition pathway – synthesis, kinetics, thermodynamics and rapid cellular internalization of a holotransferrin–maghemite nanoparticle construct. Biochim. Biophys. Acta *1830*:4254–4264.

Pitti, R. M., Marsters, S. A., Ruppert, S., Donahue, C. J., Moore, A., and Ashkenazi, A. **1996**. Induction of apoptosis by Apo-2 ligand, a new member of the tumor necrosis factor cytokine family. J. Biol. Chem. *271*:12687–12690.

Rananeh, S., and Dadras, M. R. **2015**. The possibility of using magnetic nanoparticles to increase the therapeutic efficiency of Herceptin antibody. Biomed Tech (Berl) *60*:485–490.

Riehle, R. D., Cornea, S., Degterev, A., and Torchilin, V. **2013**. Micellar formulations of pro-apoptotic DM-PIT-1 analogs and TRAIL in vitro and in vivo. Drug Deliv. *20*:78–85.

H. S. Rogers, E. R. Buhle, J. HilleRisLambers, E. C. Fricke, R. H. Miller, J. J. Tewksbury, Effects of an invasive predator cascade to plants via mutualism disruption. Nature Comm. **2017**, *8*, 14557- ….

Sachdeva, M. S. **1998**. Drug targeting systems for cancer chemotherapy. Expert Opin. Investig. Drugs *7*: 1849–1864.

Schneider, P., Bodmer, J. L., Thome, M., Hofmann, K., Holler, N., and Tschopp, J. **1997**. Characterization of two receptors for TRAIL1. FEBS Lett. *416*:329–334.

Schneider, P., Holler, N., Bodmer, J. L., Hahne, M., Frei, K., Fontana, A., and Tschopp, J. **1998**. Conversion of membrane-bound Fas (CD95) ligand to its soluble form is associated with downregulation of its proapoptotic activity and loss of liver toxicity. J. Exp. Med. *187*:1205–1213.

Seifert, O., Plappert, A., Fellermeier, S., Siegemund, M., Pfizenmaier, K., and Kontermann, R. E. **2014a**. Tetravalent antibody–scTRAIL fusion proteins with improved properties. Mol. Cancer Therapeutics *13*:101–111.

Seifert, O., Pollak, N., Nusser, A., Steiniger, F., Ruger, R., Pfizenmaier, K., and Kontermann, R. E. **2014b**. Immuno-LipoTRAIL: targeted delivery of TRAIL-functionalized liposomal nanoparticles. Bioconjug. Chem. *25*:879–887.

Song, X., Kim, H. C., Kim, S. Y., Basse, P., Park, B. H., Lee, B. C., and Lee, Y. J. **2012**. Hyperthermia-enhanced TRAIL- and mapatumumab-induced apoptotic death is mediated through mitochondria in human colon cancer cells. J. Cell. Biochem. *113*:1547–1558.

Sun, X., Pang, Z., Ye, H., Qiu, B., Guo, L., Li, J., Ren, J., Qian, Y., Zhang, Q., Chen, J., and Jiang, X. **2012**. Co-delivery of pEGFP-hTRAIL and paclitaxel to brain glioma mediated by an angiopep-conjugated liposome. Biomaterials *33*:916–924.

Walczak, H., Miller, R. E., Ariail, K., Gliniak, B., Griffith, T. S., Kubin, M., Chin, W., Jones, J., Woodward, A., Le, T., Smith, C., Smolak, P., Goodwin, R. G., Rauch, C. T., Schuh, J. C., and Lynch, D. H. **1999**. Tumoricidal activity of tumor necrosis factor-related apoptosis-inducing ligand in vivo. Nat. Med. *5*:157–163.

Wang, S. **2008**. The promise of cancer therapeutics targeting the TNF-related apoptosis-inducing ligand and TRAIL receptor pathway. Oncogene *27*:6207–6215.

Wang, Y. X., and Ng, C. K. **2011**. The impact of quantitative imaging in medicine and surgery: charting our course for the future. Quant. Imaging Med. Surg. *1*:1–3.

Whelan, J., and Mayenne, F. **2006**. Drug delivery: it's a small world. Chem. Ind.:18-20, by Park, K. 2007. Nanotechnology: What it can do for drug delivery, J Control Release. 120: 1-3.

Yoo, J., Kim, H. R., and Lee, Y. J. **2006**. Hyperthermia enhances tumour necrosis factor-related apoptosis-inducing ligand (TRAIL)-induced apoptosis in human cancer cells. Int. J. Hyperthermia *22*:713–728.

Zakaria, A. B., Picaud, F., Rattier, T., Pudlo, M., Dufour, F., Saviot, L., Chassagnon, R., Lherminier, J., Gharbi, T., Micheau, O., and Herlem, G. **2015**. Nanovectorization of TRAIL with single wall carbon nanotubes enhances tumor cell killing. Nano Lett. *15*:891–895.